Supporting information

1 Full name of materials mentioned in the main text

PM6: poly[(2,6-(4,8-bis(5-(2-ethylhexyl-3-fluoro)thiophen-2-yl)-beneo] [1,2-b:4,5-b′] dithiophene))-alt-(5,5-(1′,3′-di-2-thienyl-5′,7′-bis(2-ethylhexyl)beneo[1′,2′-c:4′,5′-c′]dithiophene 4,8-dione)

D18: Poly[(2,6-(4,8-bis(5-(2-ethylhexyl-3-fluoro)thiophen-2-yl)-benzo[1,2-b:4,5-b′]dithiophene))-alt-5,5′-(5,8-bis(4-(2-butyloctyl)thiophen-2-yl)dithieno[3′,2′:3,4;2″,3″:5,6]benzo[1,2-c][1,2,5]thiadiazole)]

Y6: 2,2′-((2Z,2'Z)-((12,13-bis(2-ethylhexyl)-3,9-diundecyl-12,13-dihydro-[1,2,5]thiadiaeolo[3,4-e] thieno [2″,3″:4′,5′]thieno[2′,3′:4,5]pyrrolo[3,2-g]thieno[2′,3′:4,5]thieno[3,2-b]indole-2,10-diyl)bis(methanylylidene))bis (5,6-difluoro-3-oxo-2,3dihydro-1H-indene-2,1-diylidene)) dimalononitrile

L8-BO: 2,2′-((2Z,2′Z)-((12,13-bis(2-ethylhexyl)-3,9-(2-butyloctyl)-12,13-dihydro-[1,2,5]thiadiazolo[3,4-] thieno[2″,3″:4′,5′]thieno[2′,3′:4,5]pyrrolo[3,2-g]thieno[2′,3′:4,5]thieno[3,2-b]indole-2,10-diyl)bis(methanylylidene)) bis(5,6-difluoro-3-oxo-2,3-dihydro-1H-indene-2,1-diylidene))dimalononitrile

PEDOT:PSS: poly(3,4-ethylenedioxythiophene): poly(styrenesulfonate)

PDINN: N,N'-Bis{3-[3-(Dimethylamino)propylamino]propyl}perylene-3,4,9,10-tetracarboxylic diimide

2 Materials

PM6 and PDINN were purchased from Solarmer Materials Inc. L8-BO was purchased from Flex PV. The molybdenum oxide (MoO_3) was purchased from Sigma-Aldrich. PEDOT:PSS was purchased from Xi'an Polymer Light Technology Corp. Toluene (Tol) and o-xylene (o-XY) were purchased from Sigma-Aldrich. ITO-coated glass substrates were purchased from South China Science & Technology Company Limited.

3 Device fabrication

Small-area OSCs were constructed with a configuration of ITO/PEDOT:PSS /Active Layer/PDINN/Ag. For the active layer, a solution was prepared using o-xylene (o-XY) or toluene (Tol) as the solvent, with a concentration of 8.8 mg/mL and a donor to acceptor ratio of 1:1.2. The ITO glass was sequentially cleaned with detergent, deionized water, and ethanol, then dried at 70 °C in a baking oven. After 15 min ultraviolet-ozone (UVO) treatment for the ITO substrate, a PEDOT:PSS layer was deposited onto the ITO-coated glass through spin-coating at 3000 r/min for 30 s. Subsequently, the active layer was fabricated using a doctor blade coater (BD Coater H100, Hunan NanoUp Electronics Technology Co., Ltd.) at a speed of 70 mm/s and annealed at 100 °C for 10 min. A PDINN/methanol solution (1.0 mg/mL) was then spin-cast on the active layer at 5000 r/min for 30 s. Finally, a silver layer (~100 nm) was thermally evaporated onto the active layers. Large-area modules were produced following similar steps as those used for the small-area OSCs. The laser scribing of module used the UV laser (LS-UN3, Hunan NanoUp Electronics Technology Co., Ltd.). For spin-coated devices, the active layer solution was prepared using chloroform as the solvent, with a concentration of 16.5 mg/mL and a donor to acceptor ratio of 1:1.2. The optimized content of 1,8-diiodooctane (DIO) is 0.25% (vol%). The active layer film was fabricated using a one-step dynamic spin-coating technique, with a rotation speed of 3500 r/min for 30 s. All other procedures remain consistent with the process outlined above.

4 Film and device characterizations

The morphologies of the blend films were investigated by atomic force microscopy (AFM, Dimension icon, Bruker, United States) using peakforce tapping mode. The Grazing-incidence wide-angle X-ray scattering (GIWAXS) was performed using Xenocs Xeuss 3.0 (France) to characterize the molecular orientation of the active layer films (test conditions: incidence angle 0.2°, detector distance 130 mm, wavelength 1.341 Å) at Vacuum Interconnected Nanotech Workstation (Nano-X) of SINANO. The in-situ UV-vis absorption spectra

measurements were conducted by PGO-100 spectrometer (Shaanxi Puguang Weishi Co. Ltd., China) for investigating the film formation. The integration time was 19 ms with automatically recorded spectra every 12 ms. The current density−voltage (*J*−*V*) characteristics of small OSC devices and small OSC modules were measured by a Keithley 2400 source meter unit under AM 1.5G (100 mW/cm^2) irradiation from a solar simulator (SAN-EI model XES-40S3). Before each test, the light intensity was calibrated with a standard Si solar cell with KG2 filter (made by Enli Technology Co., Ltd., Taiwan, and calibrated report can be traced to NREL). The *J*−*V* curves were measured from −0.07 to 0.95 V. The scan speed was fixed at 0.02 V/step. The EQE spectra were measured using a QE-R Solar Cell Spectral Response Measurement System (Enli Technology Co., Ltd., Taiwan). In the Photo-CELIV, TPC and TPV measures, the OSCs were fabricated with the same method as mentioned above. The data were obtained by the all-in-one characterization platform (Paios, Fluxim AG, Switzerland).

5 Figures and tables

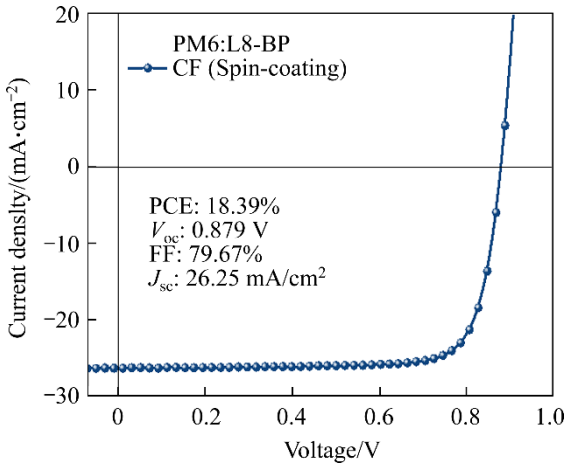

Figure S1 The *J*−*V* curve of spin-coated OSC processed with CF

Table S1 The summary of PCEs for OSC modules fabricated with non-halogenated solvents

Publication time	Solvent	Method	PCE/%	Active area/cm^2	Active layer	Ref.
2022.05	Tol	Doctor-blading	14.79	18.73	PM6: BTP-BO-4Cl	[1]
2022.10	o-XY	Slot-die-coating	14.62	7.50	PM6:T8	[2]
2022.12	o-XY	Slot-die-coating	12.20	30.00	PM6:Qx-1	[3]
2023.01	o-XY	Doctor-blading	14.42	25.20	PM6:CH7	[4]
2023.03	Tol	Doctor-blading	15.10	23.60	PBQx-TF:eC9-2Cl	[5]
2023.07	Tol	Doctor-blading	15.20	18.73	PM6:L8-BO	[6]
2023.09	Tol	**Spin-coating**	16.26	19.30	PM6:PBQx-TCl:PY-IT	[7]
2023.10	o-XY	Slot-die-coating	13.25	46.20	PM6/G-Trimer	[8]
2023.10	o-XY	Bar-coating	13.88	55.00	PM6:NAP-TT-SiBTZ:Y7	[9]
2024.03	o-XY	Doctor-blading	15.10	211.40	PM6:Y6-C12:PC61BM	[10]
2024.04	**o-XY**	**Doctor-blading**	**16.07**	**11.68**	**PM6:L8-BO**	**This work**

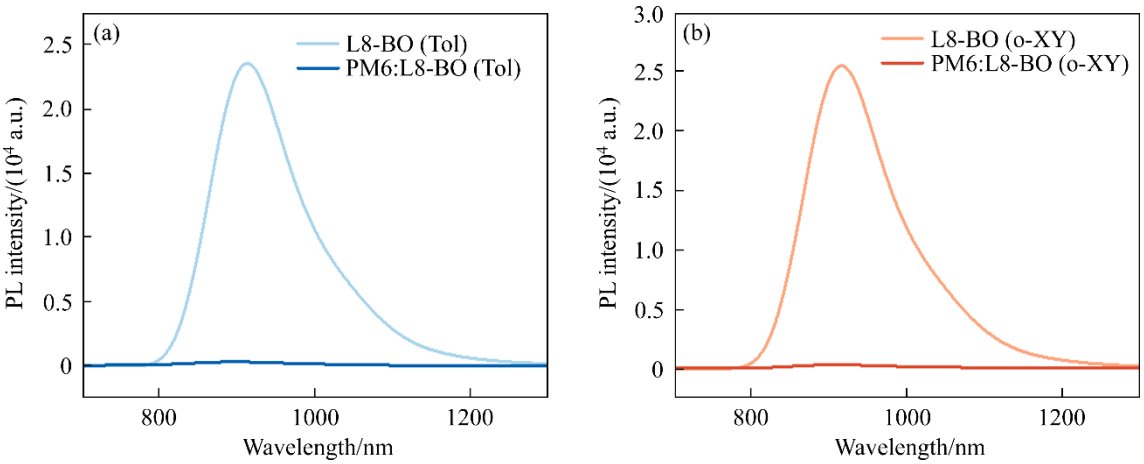

Figure S2 Photoluminescence (PL) spectra of pure L8-BO films and PM6:L8-BO blend films processed with (a) Tol and (b) o-XY

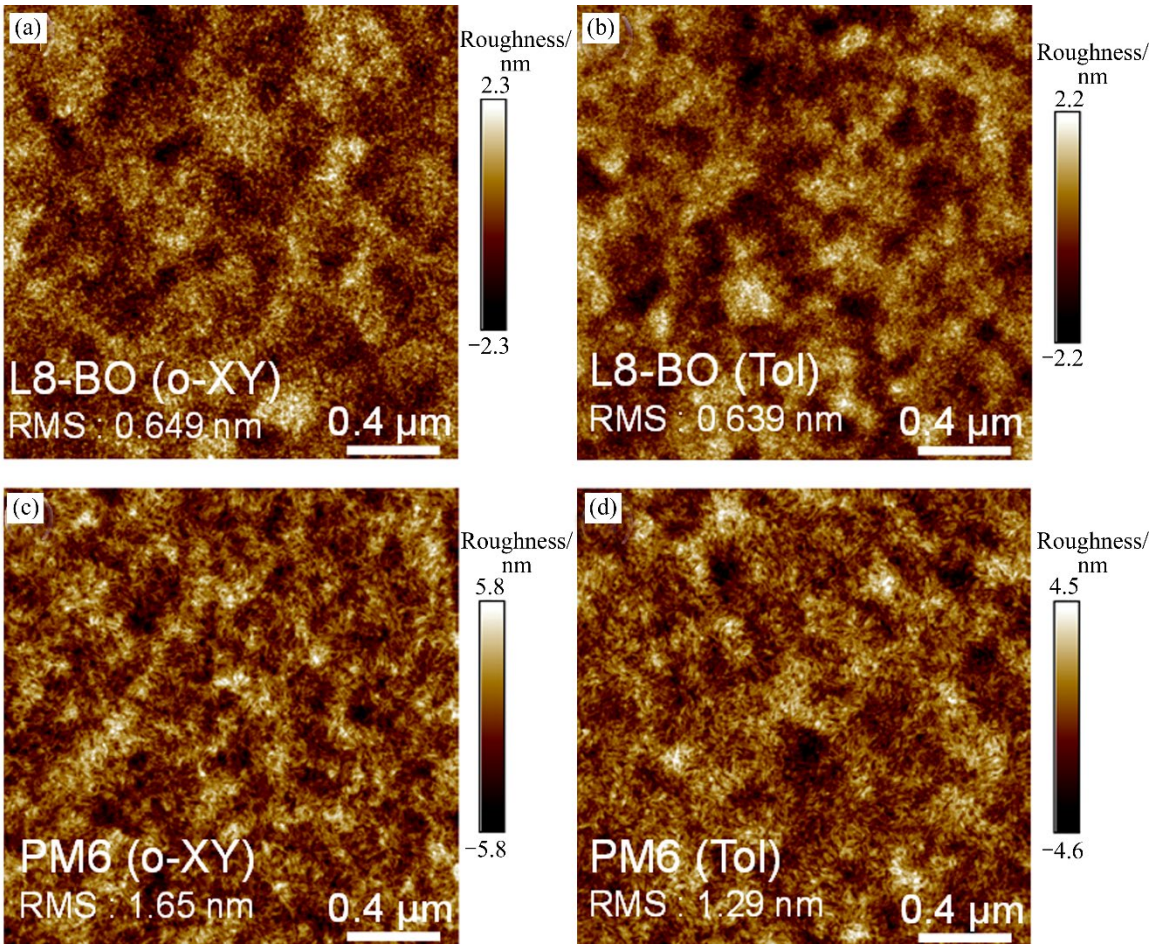

Figure S3 AFM images of L8-BO films processed with (a) o-XY and (b) Tol; AFM images of PM6 films processed with (c) o-XY and (d) Tol

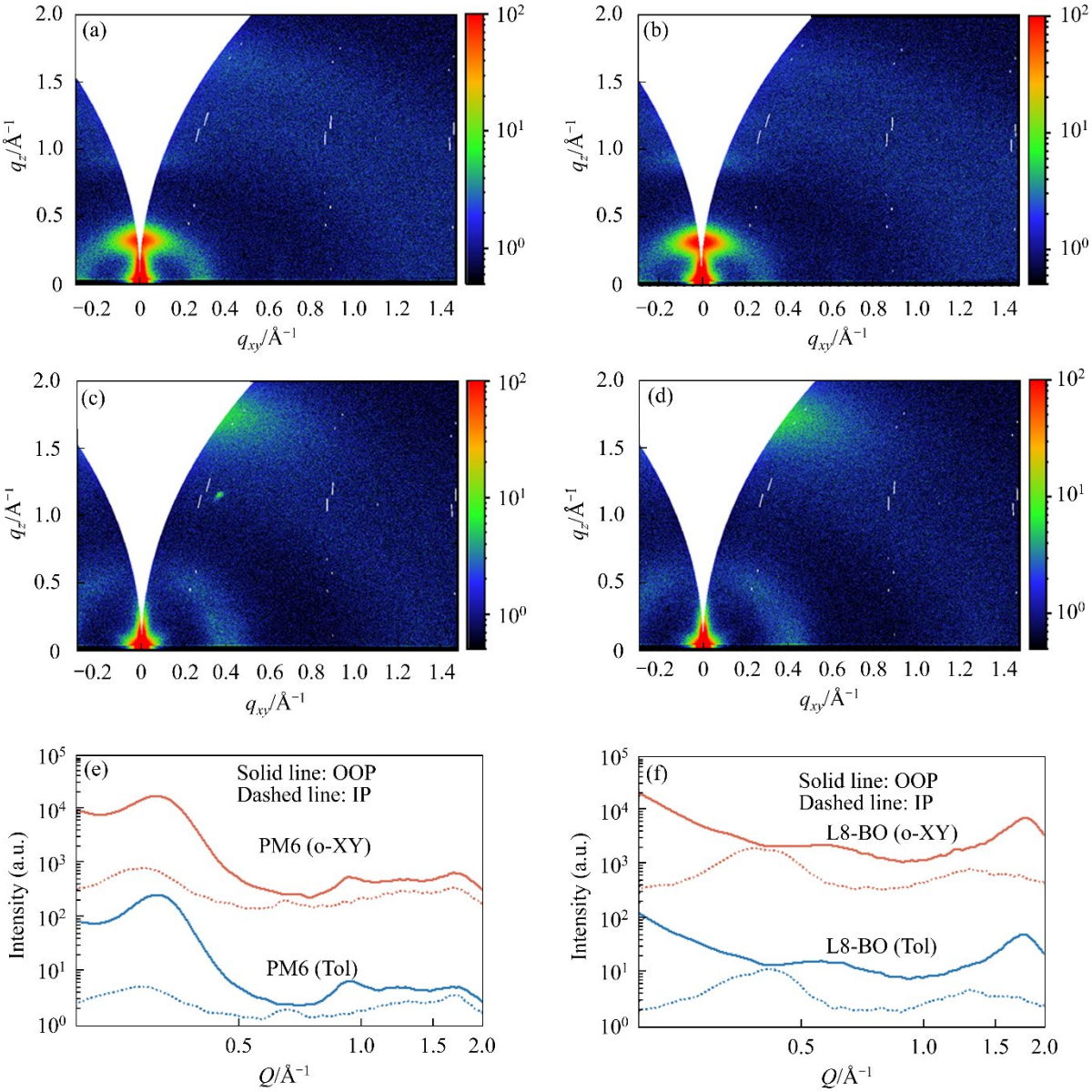

Figure S4 2D GIWAXS patterns of PM6 thin films processed with (a) o-XY and (b) Tol; 2D GIWAXS patterns of L8-BO thin films processed with (c) o-XY and (d) Tol; (e) The GIWAXS lines profiles of PM6 thin films processed with different solvents; (f) The GIWAXS line profiles of L8-BO thin films processed with different solvents

Table S2 Structure parameters of (010) peak for neat and blend films with out-of-plane direction

Material	Solvent	q^a/Å^{-1}	d-spacing^b/Å^{-1}	FWHM^c/Å^{-1}	CCL^d/Å^{-1}
PM6:L8-BO	o-XY	1.753	3.585	0.338	16.735
PM6:L8-BO	Tol	1.748	3.595	0.377	15.007
PM6	o-XY	1.704	3.688	0.427	13.237
PM6	Tol	1.686	3.727	0.445	12.716
L8-BO	o-XY	1.774	3.541	0.370	15.266
L8-BO	Tol	1.750	3.591	0.379	14.907

Note: [a] Obtained from the original data; [b] Calculated from the equation: d-spacing=$2\pi/q$; [c] Obtained from the fitting patterns of line-cut profiles; [d] Calculated from the Scherrer equation: CCL=$2\pi k$/FWHM, where FWHM is the full-width at half-maximum of the peak and k is a shape factor (here we use 0.9).

Table S3 Structure parameters of (100) peak for neat and blend films with in-plane direction

Material	Solvent	q^a/Å^{-1}	d-spacing^b/Å^{-1}	FWHM^c/Å^{-1}	CCL^d/Å^{-1}
PM6:L8-BO	o-XY	0.310	20.281	0.113	50.203
PM6:L8-BO	Tol	0.313	20.081	0.116	48.703
PM6	o-XY	0.293	21.433	0.112	50.351
PM6	Tol	0.290	21.687	0.117	48.448
L8-BO	o-XY	0.403	15.600	0.166	34.008
L8-BO	Tol	0.411	15.297	0.158	35.845

Note: [a] Obtained from the original data; [b] Calculated from the equation: d-spacing=$2\pi/q$; [c] Obtained from the fitting patterns of line-cut profiles; [d] Calculated from the Scherrer equation: CCL=$2\pi k$/FWHM, where FWHM is the full-width at half-maximum of the peak and k is a shape factor (here we use 0.9).

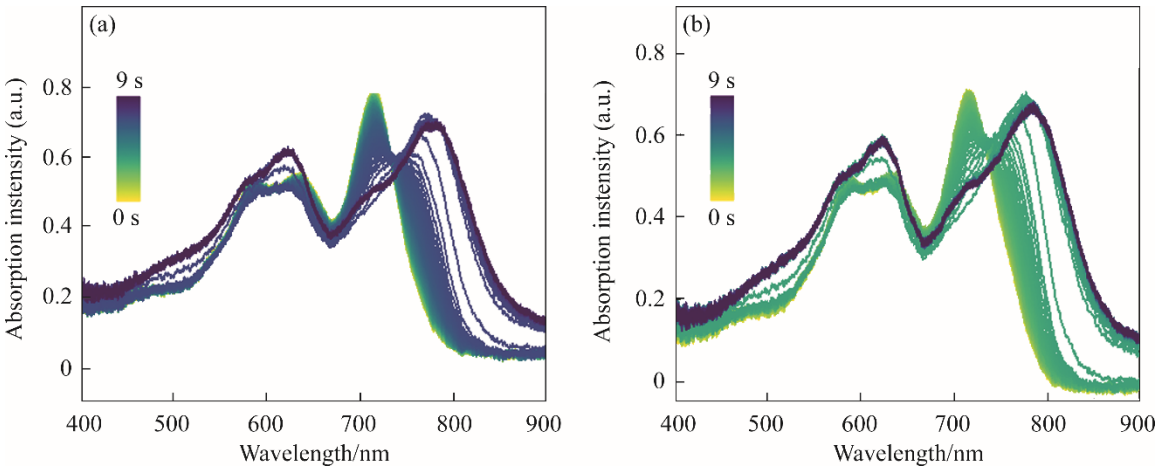

Figure S5 Time evolution of UV-vis absorption line profiles of PM6:L8-BO thin films processed with (a) o-XY and (b) Tol

References

[1] FAN Jing-yuan, LIU Zhi-xi, RAO J, et al. High-performance organic solar modules *via* bilayer-merged-annealing assisted blade coating [J]. Advanced Materials, 2022, 34(28): e2110569. DOI: 10.1002/adma.202110569.

[2] SUN Rui, WANG Tao, YANG Xin-rong, et al. High-speed sequential deposition of photoactive layers for organic solar cell manufacturing [J]. Nature Energy, 2022, 7: 1087−1099. DOI: 10.1038/s41560-022-01140-4.

[3] SHEN Yi-fan, ZHANG Hao, ZHANG Jian-qi, et al. In situ absorption characterization guided slot-die-coated high-performance large-area flexible organic solar cells and modules [J]. Advanced Materials, 2023, 35(10): e2209030. DOI: 10.1002/adma.202209030.

[4] ZHANG Shu-chao, CHEN Hong-bin, WANG Pei-ran, et al. A large area organic solar module with non-halogen solvent treatment, high efficiency, and decent stability [J]. Solar RRL, 2023, 7(7): 2300029. DOI: 10.1002/solr.202300029.

[5] WANG Jian-qiu, WANG Ya-fei, BI Peng-qing, et al. Binary organic solar cells with 19.2% efficiency enabled by solid additive [J]. Advanced Materials, 2023, 35(25): e2301583. DOI: 10.1002/adma.202301583.

[6] XIANG Jia-le, LIU Zhi-xi, CHEN Hong-zheng, et al. Robust and sustainable indium anode leading to efficient and stable organic solar cells [J]. Advanced Materials, 2023, 35(39): e2303729. DOI: 10.1002/adma.202303729.

[7] CHEN Tian-yi, ZHENG Xiang-jun, WANG Di, et al. Delayed crystallization kinetics allowing high-efficiency all-polymer photovoltaics with superior upscaled manufacturing [J]. Advanced Materials, 2024, 36(3): e2308061. DOI: 10.1002/adma.202308061.

[8] WANG Cai-xuan, MA Xiao-ming, SHEN Yi-fan, et al. Unique assembly of giant star-shaped trimer enables non-halogen solvent-fabricated, thermal stable, and efficient organic solar cells [J]. Joule, 2023, 7(10): 2386−2401. DOI: 10.1016/j.joule.2023.09.001.

[9] GOKULNATH T, KIM H, LEE J, et al. High performance air-processed organic photovoltaic modules (~55 cm^2) with an efficiency of >17.50% by employing halogen-free solvent processed polymer donors [J]. Advanced Energy Materials, 2023, 13(46): 2302538. DOI: 10.1002/aenm.202302538.

[10] BASU R, GUMPERT F, LOHBREIER J, et al. Large-area organic photovoltaic modules with 14.5% certified world record efficiency [J]. Joule, 2024, 8(4): 970−978. DOI: 10.1016/j.joule.2024.02.016.